Received: 22 July 2024 | Revised: 12 September 2024 | Accepted: 3 October 2024

DOI: 10.1049/rpg2.13135

IET Renewable Power Generation

The Institution of Engineering and Technology WILEY

ORIGINAL RESEARCH

Towards the development of offshore wind farms in the Mediterranean Sea: A techno-economic analysis including green hydrogen production during curtailments

Riccardo Travaglini[1] | **Francesco Superchi**[1] | **Francesco Lanni**[2] | **Giovanni Manzini**[2] | **Laura Serri**[2] | **Alessandro Bianchini**[1]

[1]Department of Industrial Engineering, University of Florence, Firenze, Italy

[2]Ricerca sul Sistema Energetico - RSE S.p.A., Milano, Italy

Correspondence
Alessandro Bianchini, Department of Industrial Engineering, University of Florence, Via di Santa Marta 3, Firenze, Italy.
Email: alessandro.bianchini@unifi.it

Funding information
Research Fund for the Italian Electrical System under the Three-Year Research Plan 2022–2024, Grant/Award Number: DM MITE n. 337, 15.09.2022

Abstract

Bringing floating offshore wind turbines (FOWTs) to a real industrial maturity and reducing the levelized cost of floating wind energy are key to significantly increasing the penetration of renewables in the energy mix of Mediterranean countries, especially if in combination with suitable energy storage systems, such as those involving green hydrogen production. The present study analyses techno-economic aspects of some of the technologies related to FOWTs and hydrogen production by means of offshore-generated energy, aiming to evaluate the potential of a floating wind farm integrated with a power-to-gas energy storage system in a specific installation site near the Sardinian shores. In comparison to the pioneering studies to date, a more detailed computational model is used, able to account for several critical factors like a better description of metocean conditions, constraints on grid capacity, and a state-of-the-art model to define the farm layout. Concerning hydrogen production, a comparison between the statistical approach, which is commonly used in the field, and a fully time-dependent method is performed. Proposed results obtained with the statistic and the time-dependent approach show values ranging between 3.79 and 5.47€/kg, respectively. These outcomes are thought to provide an interesting comparison between different fidelity approaches and realistic reference values for the levelized cost of hydrogen by floating wind in the Mediterranean Sea.

1 | INTRODUCTION

Floating Offshore Wind Turbine (FOWT) technology is still at a pre-commercial stage, with just a few demonstrators deployed and two farms in operation. Moreover, none of these plants is located in the Mediterranean Sea due to the challenging metocean conditions [1], the complexity of maritime space, and the uncertainty in the regulatory framework. According to [2], at the end of 2021 floating wind accounts for just 0.1% of overall offshore wind, but it should rise to 6.1% of all new installations with an estimated 16.5 GW of new capacity by 2030. A large fraction of the new installed power is expected from floating installations in the Mediterranean Sea, but the feasibility and sustainability of these new projects may be affected by the scarcity of reference data regarding capital and operational expenditures (CAPEX and OPEX, respectively), metocean conditions, and power transportation by subsea cables. Beyond FOWT technology itself, another key issue to be tackled is how the expected power can be handled by existing grids in the Mediterranean Sea, some of which could not be ready to accept punctual large power fluxes brought onshore by offshore cables. Therefore, novel offshore wind farms will need to manage possible energy curtailments, which involve the planned reduction of the power output to prevent overloads and grid congestions. To this end, different strategies can be investigated. One of such strategy that is receiving attention involves the production of green hydrogen from energy surplus, which has the potential to increase green energy production. Compared to batteries,

green hydrogen is a versatile energy carrier that can be used for long-term storage, both in liquid and gaseous phases, and can act both as a fuel for various applications, including fuel cells or combustors, and as a key element in industrial processes in the so-called hard-to-abate sectors [3]. However, few research efforts have been spent on the exploitation of curtailments from FOWT farms in the Mediterranean Sea, and in general on the production of Hydrogen to reduce the associated energy wastes. Specifically, Wang et al. [4] evaluated the feasibility of producing hydrogen from curtailments of renewable energy sources (RES) in order to feed fuel cells electric vehicles. The analyses show that the use of electrolysis can provide relevant benefits to mitigate the effects of intermittency of RES. In their study, Park et al. [5] demonstrated how comprehensive system modeling can be used to assess the economic viability of producing green hydrogen from curtailed solar and onshore wind renewable energy using actual meteorological data. Results show an LCOH of around 5.9$/kg, consistent with the findings of this study. In [6], McDonagh et al. showed that the coupling of Offshore wind farms and electrolysis has a good potential to increase the revenues of a plant thanks to the exploitation of curtailed power. The findings depict an LCOH of 3.77€/kg for a wind farm located in the Irish Sea. Biggins et al. [7] proposed a stochastic optimization to maximize the revenues of a system composed by wind farms, batteries and electrolyzers. Results show that hydrogen production increases the average revenue and curtailed wind utilization significantly more than the Li-ion battery. However, although many research efforts were spent to evaluate hydrogen production costs from wind power, in most of these studies a simplified model to convert electricity into hydrogen is used. The adoption of a conversion factor, such as the one adopted by Yan et al. in [8], may result in relevant overestimation of the producibility. Finally, Gambou et al [9] highlighted that relying solely on efficiency-based models is insufficient and that more comprehensive approaches incorporating the stack degradation processes are needed to properly simulate long period time spans. While the simple models can be useful for initial design and analysis, they cannot accurately capture the thermal behavior of the electrolyzer [10].

Within the framework of large-scale commercialization of floating offshore farms foreseen to take place between 2030 and 2050, and given the targets set by the Italian government in the National Integrated Climate and Energy Plan [11], the present study aims to provide projections on the Levelized Cost of Energy (LCOE) associated with these farms in the Mediterranean Sea, so as to evaluate the feasibility of existing scenarios and provide an insight into the potential economic viability. Additionally, the purpose of the performed analyses is to estimate the Levelized cost of Hydrogen (LCOH) obtained by exploiting the energy from curtailments. To this end, a comparison between a simplified and a more complex electrolyzer model is provided. Compared to the mentioned studies, a more detailed model allows considering the effects of temperature variation and aging of the stack. The adoption of a time-dependent approach in turn enables the evaluation of the exploitability of the power input, leading to more accurate cost estimations.

TABLE 1 Wind turbines data—Github.com/IEAWindTask37.

Wind turbine	IEA 10 MW	IEA 15 MW
Hub height [m]	119	150
Rotor diameter [m]	198	242
Rated power [MW]	10	15
Cut in/out wind speed [m/s]	4/25	3/25
Rated wind speed [m/s]	10.8	10.6

The first part of the work presents the methods used to assess the performance and evaluate the costs of floating offshore wind turbines and electrolyzers, as well as the associated technologies, including substructures, submarine high-voltage cables, and floaters. Then, a specific test case, located near the shores of Sardinia, is analyzed from a producibility point of view. Western Sardinia is one of the most interesting marine areas for the future deployment of offshore wind in Italy. Many projects at different authorization stages already insist on this area. This test case is used to benchmark the proposed simulation model with the existing pioneering studies on the topic that were based on more simplified assumptions. To this end, a comparison is made between the results deriving from the statistical analysis based on the aggregated power and hydrogen production and those obtained with a time-dependent approach in order to assess the effects of the temporal sequence of curtailments on the final production and cost. Finally, adopted economic models are discussed, together with known data for the cost ranges of the main technologies. These are finally used to derive estimations of the potential farm performance in terms of Annual Energy Production (AEP), LCOE, and LCOH.

2 | METHODS

2.1 | Wind turbines

The current study considers the two reference wind turbines (WTs) proposed by the IEA for offshore installations, characterized by a design power of 10 and 15 MW, respectively. This selection is consistent with the focus being put on a time scale beginning in 2030 when it is foreseen that these turbine sizes will have attained maturity and undergone extensive commercialization. While further upscaling of wind turbine size can lead to technical improvements, the large-scale diffusion of generators with a nominal power higher than 15 MW is not realistic before 2030 [12].

Table 1 highlights the main parameters of the IEA 10 and 15 MW, while the associated power and thrust curves needed for the AEP estimation are displayed in Figure 1. While NREL established a lifespan of 25 years for the two wind turbines under examination, this study incorporates a lifetime of 30 years. This assumption was based on some recent findings [13, 14], which indicated that the turbines could continue functioning for an additional five years with planned extraordinary maintenance, without any significant loss in performance. Through

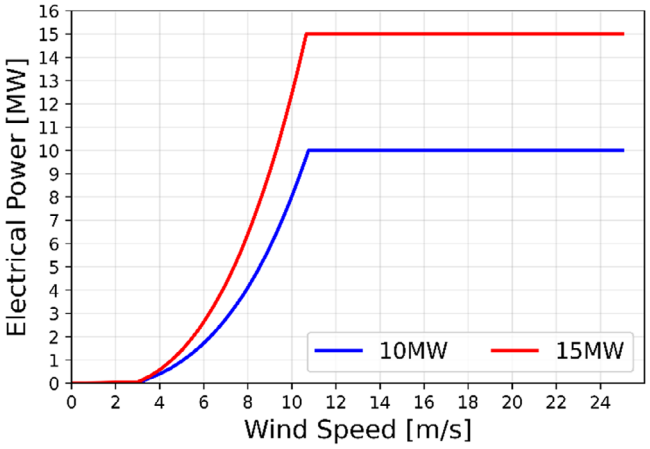

FIGURE 1 Power curve of IEA 10 and 15 MW turbines.

an assessment of the technology readiness level and feasibility projections for various existing floating platforms, the semi-submersible floater has emerged as the most promising option for installations within the Mediterranean Sea [15]. The semi-submersible platform has been deemed the most suitable trade-off between stabilization for buoyancy and ballast, especially considering significant sea depths and metocean conditions characteristic of the most promising sites within the Mediterranean Sea. Concerning the mooring system, two configurations are commonly used, namely the catenary and the semi-taut systems [16, 17]. This study has opted to employ the catenary type, linking each turbine to the seabed through three mooring lines. With regard to energy delivery to shore, the electric layout comprises intra-array dynamic cables that connect the FOWTs to the substation, as well as export cables.

The optimization of the electrical configuration of the wind farm herein considers configurations with eight 10 MW and six 15 MW turbines, respectively. This arrangement was due to the limitation of selected intra-array cables, which have a design voltage of 66 kV and a capacity of 90 MVA. As a result, the length of the intra-array cables is a key parameter that affects the capital expenditures of the wind farm. This length is computed using the equation presented below.

$$L_{CABLE} = 2 * d_{SEA} * 2.6 + L_T. \quad (1)$$

This equation takes into account that the turbine distance (L_T) must be added to the sea depth (d_{SEA}) increased by a factor of 2.6, as reported in [18]. Regarding the transmission system, both high-voltage direct (HVDC) and alternating current (HVAC) cables were considered and compared to determine the optimal choice. For this specific installation site, situated 42 km from the onshore electricity delivery point, the most cost-effective solution was found to be the deployment of HVAC cables [19]. This technology has lower fixed costs, but higher costs per unit length due to the significant increase in cable sectional area to compensate for reactive power. On the other hand, HVDC cables have higher fixed costs and lower cost per unit length, thus becoming convenient for distances approximately longer than 60 km [20–23]. The length of submarine transmission cables is again estimated using Equation (1) by replacing L_T with the export distance. Due to the fixed substation location, this length is equal to 43.77 km for all configurations.

TABLE 2 Selected wind farm layout spacing description.

Farm layout	10 MW WTs farm [km]	15 MW WTs farm [km]
Square 5d-5d	0.99–0.99	1.20 × 1.20
Square 7d-7d	1.39 × 1.39	1.68 × 1.68
Rectangular 10d-5d	1.98 × 0.99	2.40 × 1.20
Rectangular 10d-7d	1.98 × 1.39	2.40 × 1.68
Square 10d-10d	1.98 × 1.98	2.40 × 2.40

2.2 | Wind farm layout and installation site

This study focuses on an area situated approximately 40 km from the northwest shores of Sant'Antioco, an island near Sardinia. Despite other projects being presented to the Italian authorities in this area, the purpose of this work is to estimate the LCOE for a wind farm with the potential integration of hydrogen production in a timeline starting from 2030. Despite the relatively fewer restrictions on surface occupancy, the lower noise pollution, and the higher distance from human activities for offshore wind turbines in contrast to onshore installations, the optimal layout of offshore wind farms poses significant challenges, including submersible static and dynamic intra-array cables and moorings. Moreover, the AEP is strongly affected by turbine wakes, which reduce the wind generators' producibility and the potential revenue from the farm. For these reasons, this study presents a sensitivity analysis based on the distance between the FOWTs, reported as turbine diameter (Table 2), to evaluate how wakes affect the AEP and the resulting LCOE, balancing the increasing CAPEX. To optimize the farm shape, two different layouts were considered and compared: a square and a rectangular one, the latter depicted in Figure 2. Moreover, the environmental footprint of the wind farm is depicted by its extension. In this case, the sea lot occupied ranges from 77.8 to 317 km2. The performance of each layout was evaluated and compared by analyzing the configurations presented in Table 2. In this study, the orientation of the cluster of rotors was optimized to maximize energy capture while minimizing wake effects on downstream wind generators, considering the prevalent wind direction from the northwest, as shown in Figure 2. Wind farms are composed of one hundred 10 MW turbines and sixty-seven 15 MW turbines, for a farm rated power of 1 GW and 1.005 GW, respectively.

2.3 | Power-to-hydrogen

Current literature considers three main types of power-to-hydrogen configuration, classified by the electrolyzer location [24]:

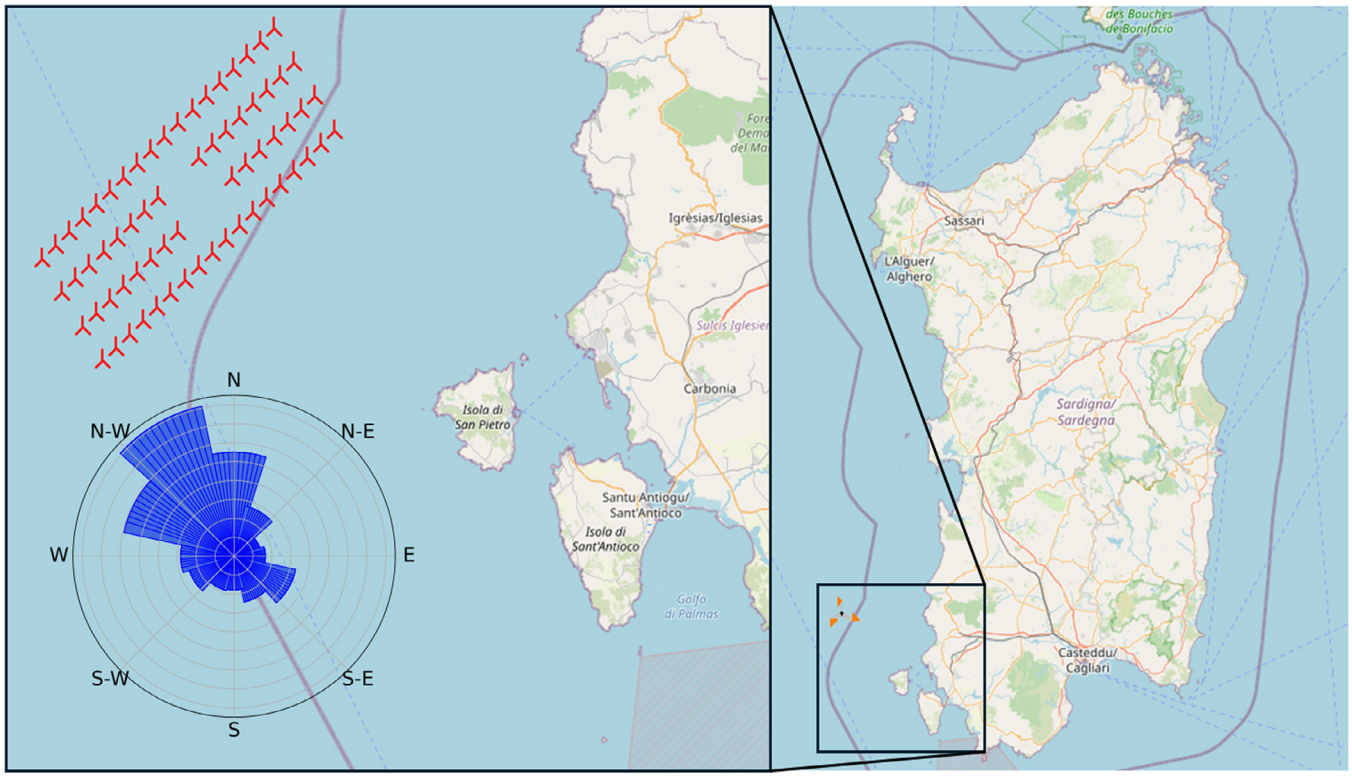

FIGURE 2 An example of a 10 MW WTs farm configuration (Rectangular 10d-7d) and wind rose of the considered area.

- directly on the same platform as the wind turbine;
- on an offshore substation;
- onshore close to the point of delivery of electricity.

The first configuration, referred to as "decentralized offshore", makes use of smaller, independent electrolyzers, which contribute to a more resilient system and a reduced land footprint. However, this approach needs high capital investment and leads to reduced system efficiency, mainly due to the highly variable power input from individual turbines. The produced hydrogen is transported via flexible pipelines to an offshore central substation and then channeled onshore as the only energy vector. The second option, commonly referred to as "centralized offshore", involves the collection of electricity at an offshore substation, where hydrogen is produced and then transported to the shore via rigid pipelines. This approach enables the creation of a hybrid energy vector. In the present study, the third configuration, which utilizes electricity as the sole energy vector towards the shore and involves electrolysis near the delivery location, has been selected. Despite the land footprint for the hydrogen production system, the "centralized onshore" approach is characterized by a higher technology readiness level and lower CAPEX. This configuration, in fact, relies upon mature technologies and simplifies both plant maintenance and supply of fresh water. Moreover, it has some specific advantages like (i) allowing the selection of electrolyzers relying only on performance and cost, with no constraint on size, resistance to marine environment, and dynamic performance; (ii) avoiding hydrogen transportation in pipelines; (iii) producing hydrogen closer to possible users. Finally, considering that the main purpose of the wind farm is to provide electricity to the grid, while hydrogen represents only a side product, the installation of the electrolysis facility offshore would lead to a cost increase. The combined installation of electrical cables and pipelines would nullify the economic benefit of delivering hydrogen as the only energy vector.

2.4 | Wind data

Accurate evaluation of the wind resource is always critical for the proper computation of the AEP of wind energy systems. This task is even more complicated in the case of offshore installations, where the harsh environmental conditions make the installation and maintenance of floating measurement stations demanding, thus leading to a lack of measured wind data. The wind speed data used in this study were downloaded from AEOLIAN [25], a Web-GIS developed by RSE with a resolution of 1 h. Data provided by this atlas are computed from the mesoscale ones, also interpolating actual measurements performed in some points of the considered area. While the tool can provide only wind speed profiles, other parameters such as wind direction, air temperature, and humidity are essential for accurately evaluating wake effects and wind turbine power curve corrections. These parameters were then obtained from ERA5, a climate database developed by the Copernicus Climate

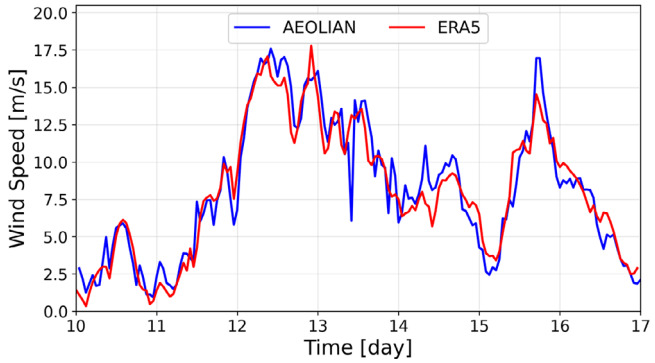

FIGURE 3 ERA5 and AEOLIAN wind speed comparison (05/2019) at 100 m.

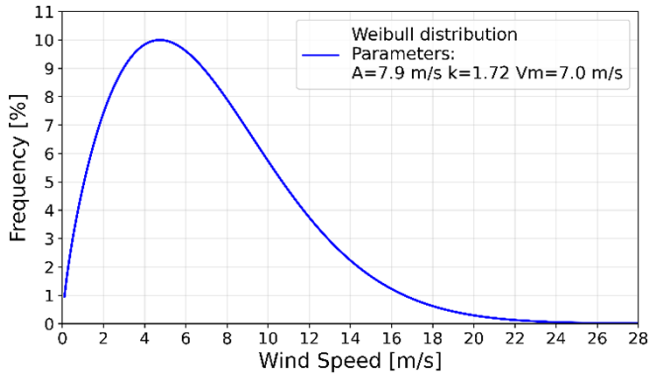

FIGURE 4 AEOLIAN Weibull distribution at 100 m.

Change Service [26]. As offshore sites are assumed to have no obstacles and low surface roughness, these parameters can be reasonably considered similar across different atlases. To validate this assumption, a comparison of the wind speed series is presented in Figure 3, which in fact shows a nice agreement between the two. The decision to use AEOLIAN data was made due to its higher spatial resolution for the available data, that is, 1 × 1 km grid with respect to 9 × 9 km of ERA5, for the Mediterranean Sea, particularly in areas near Italian shores.

Upon examination of the wind rose (Figure 2), the prevalent wind direction at the installation site is northwest, considering both wind frequency and energy.

Therefore, as depicted in Figure 2, the wind park is oriented accordingly to minimize wake losses and maximize the AEP. The Weibull shown in Figure 4 highlights a quite low shape parameter that shifts the curve to lower speed values and a mean speed of 7.0 m/s.

To match the hub height of the wind turbines -119 and 150 m for the 10 MW and 15 MW, respectively-, AEOLIAN wind speed data were extrapolated from 100 m above sea level (asl) using a scaler based on the wind shear power law proposed by default in windPRO [27]. It is important to note that the wind direction was considered at a height of 100 m asl (available in the ERA5 database), assuming it constant up to the hub height.

2.5 | windPRO calculations

windPRO [27] is a widely adopted tool for the design, development, and assessment of wind projects. In this study, the time-dependent analysis was used to evaluate the wind production trend starting from available historical wind data. Dealing with an offshore site, orography, and roughness are not significant; a surface roughness of 0.0002 m was estimated [28]. The use of windPRO instead of more simplified approaches allowed for a much more accurate evaluation of the losses due to turbine wakes. The wake model by N.O. Jensen [29], based on the assumption of a linearly expanding wake diameter with the conservative fixed wake decay coefficient of 0.06 was used as per standard practice in literature for offshore installations [30–32]. Moreover, to account for possible losses during the plant operativity, such as electrical losses and the annual availability of wind generators, the AEP was reduced by an additional 10%. Based on the authors' experience, this is quite realistic data, and it was then used for the LCOE and LCOH estimations.

2.6 | Curtailments

Curtailment is the planned reduction of wind turbine power output when the electrical grid reaches the maximum power transmission capacity. Since curtailments in Mediterranean countries predominantly affect unscheduled renewable energy sources, the widespread adoption of these sources in the "Global ambition Italia" scenario forecasted by TERNA for 2040 [33] results in a total of 11 TWh/year of curtailed energy, corresponding to approximately 5% of the predicted renewable energy production. However, this percentage should be considered indicative, as grid capacity varies significantly between different regions. Notably, the Sardinian grid near the wind farm installation site analyzed in this study has low capacity. Thus, in this study, three scenarios that vary the curtailment from 5% to 10% or 15% were considered. Furthermore, the scheduled power output reduction is modeled in two different ways:

- as a percentage of the AEP (S1), to assess the hydrogen producibility with a statistical approach,
- using a time-dependent method based on an electrolyzer model (S2).

The link between those scenarios is the constraint on the yearly curtailed energy, which is the same in both scenarios. Although the energy available for hydrogen production is unchanged, the input power in S1 is considered constant during the year for simplicity, which leads to overestimating the capacity factor (CF) of the system.

Conversely, S2 allows to introduce an electrolyzer model capable of considering variable efficiency, minimum loads, and dependence on temperature. This second approach was divided into two different sub-cases. In S2-a, considering grid congestions due to intermittent renewables, curtailments are scheduled throughout daylight hours with the power reduction shown in

TABLE 3 Wind farm power reduction in the considered curtailment scenarios.

Curtailment scenario	S1	S2-a
5% AEP	5%	10.05%
10% AEP	10%	20.10%
15% AEP	15%	30.15%

Table 3. Here, hydrogen is produced only by exploiting the energy curtailed according to the grid operation, even if this assumption leads to a sub-optimal use of the installed electrolyzer. Relying on the optimal sizes obtained in this scenario, S2-b aims to maximize the electrolyzer CF and reduce the LCOH in a 'hydrogen-driven' test case. To this end, in an attempt to achieve the operation of the electrolyzer at rated capacity for 24 h a day, the power in addition to that derived from curtailments is withdrawn from the wind farm, following an approach similar to [3].

2.7 | Electrolyzer modeling

For the scope of the present study, the annual energy input to the electrolyzers was computed as a fraction of the AEP, but two approaches were considered: the aggregated and the time-dependent ones. Due to the assumption of constant power input to the electrolyzer, the first one is quite simplified, but provides an indicative value of the cost of hydrogen produced from the wind source in the area of interest. On the other hand, the time-varying approach allows to consider the minimum power input and the variable efficiency depending on operating conditions. To assess the impact of the electrolyzer system size, a sensitivity analysis was conducted by varying the size between 10 and 60 MW. This range was selected based on some preliminary analyses, which showed that these dimensions are optimal for a 1 GW power plant within the described scenarios. Although the maximum power available for the electrolysis facility—about 300 MW- is higher than the 60 MW considered, the limited amount of time when that power occurs leads to smaller optimal capacities. Given the lack of spatial constraints and the constant power input resulting from the centralized onshore configuration, the alkaline electrolyzer (ALK) technology was here considered. In S1, to account for technology development by 2030, the efficiency of the systems was set to a fixed value of 17.98 kg/MWh [34], corresponding to an electrical efficiency of approximately 60%. On the other hand, for S2-a and S2-b the computational model of the electrolyzer described in [35] was adopted, setting the time step size to 1 h. Within this timeframe, one can estimate the efficiency variations relying on the estimation of the overpotentials due to losses. Values of current density equal to 10 kA/m^2 and voltage of 1.89 V were considered as design parameters of the cell. To carry out the economic analysis and calculate the LCOH, a 30-year timespan was assumed for the electrolyzer, with a stack replacement after 15 years (based on authors' experience), costing 40% of the CAPEX. Moreover, this study assumes that curtailed renewable energy, which would otherwise be wasted, is used to produce green hydrogen in S1 and S2-a. This assumption allows to focus solely on the expenditures associated with the electrolysis plant, neglecting hydrogen storage and pipelines due assumption of direct use near the production area. Therefore, electricity expenses were accounted for relying on the scenario:

- in S1 and S2-a energy is valued as the feed-in tariff assumed (0% or 50% of the LCOE).
- in S2-b the additional energy required is priced as the plant LCOE.

While the energy costs considered in the S2-b are unrealistic, the analysis aimed to give an idea of the theoretical minimum LCOH in a hydrogen-driven scenario.

2.8 | Metrics for cost estimation

The evaluation of costs associated with the production of electricity and hydrogen constitutes a key component of this study. Specifically, the levelized costs of energy or hydrogen are employed as the primary metrics for conducting economic analyses and represent the price at which energy and hydrogen must be sold to recover the cost of system installation and operation during the plant's lifetime. Notably, these metrics are among the most widely used in literature for this purpose.

2.8.1 | Levelized cost of energy

The present study employs the levelized cost of energy as a parameter for evaluating the costs associated with electricity generation from the offshore wind farm. This metric offers a comprehensive means of assessing all factors that influence electricity production costs, including the CAPEX and OPEX. The LCOE is determined by calculating the ratio between the discounted sum of costs projected throughout the lifespan of the plant and the actualized sum of energy that the plant will generate within the same timeframe. Since the energy generated comes from a renewable source, fuel costs are here excluded. To evaluate the cost of energy, given the variability of cash flows over the plant's lifespan, the standard definition of LCOE was adopted (Equation 2).

$$\mathrm{LCOE} = \frac{\sum_{t=1}^{n} \frac{(\mathrm{CAPEX}_t + \mathrm{OPEX}_t)}{(1+i)^t}}{\sum_{t=1}^{n} \frac{E_{prod,t}}{(1+i)^t}}. \quad (2)$$

2.8.2 | Levelized cost of hydrogen

Similar to LCOE, LCOH allows for the consideration of all parameters related to hydrogen production, facilitating comparison between different production systems. LCOH is determined with the standard expression (Equation 3) by

TABLE 4 CAPEX for the case study.

Component	10 MW WTs farm [M€/MW]	15 MW WTs farm [M€/MW]
Wind turbines	1.027	1.034
Platform	0.690	0.696
Intra array cables	0.263	0.213
Export cables	0.486	0.486
Moorings	0.112	0.105
Installation	0.169	0.169
Total	2.747	2.703

calculating the ratio between actualized cash flow and hydrogen production. This metric thus represents the cost at which hydrogen must be sold to match the production costs.

$$\mathrm{LCOH} = \frac{\sum_{t=1}^{n} \frac{(\mathrm{CAPEX}_t + \mathrm{OPEX}_t)}{(1+i)^t}}{\sum_{t=1}^{n} \frac{H_{2,prod,t}}{(1+i)^t}}. \quad (3)$$

In this work, interest rate values (i) of 5%, 7%, and 9% are chosen to carry out a sensitivity analysis.

2.8.3 | Component costs

The accurate estimation of capital and operational expenditures is crucial for computing the LCOE and LCOH of a wind farm. However, due to the limited number of existing plants, estimating the actual and projected costs of floating offshore wind turbines (FOWTs) and floating platforms is complex. In this section, all the economic data used in our analysis as specific costs that depend on the size of the wind farm are reported. Moreover, to address the uncertainty of hydrogen production costs in a 2030 scenario, data are presented in box and whiskers plots. To estimate the capital expenditures of FOWTs and floating platforms, values computed from the costs reported in the literature, for example in [36, 37], which are 1.027 and 1.034 M€/MW for 10 and 15 MW wind turbines, respectively, and 0.69 and 0.696 M€/MW for the floaters, were used. To account for the size of the wind farm, a scale factor that reduces the costs as the number of installed turbines increases was included [38]. These components, in the analyzed case study, along with the intra-array cables, constitute more than 70% of the total plant cost breakdown. To estimate intra-array cable costs, the mean value of the data reported in [36, 37, 39–41] was chosen, resulting in a specific cost of 745 k€/km. A normalized cost on the plant capacity for each wind farm was computed, as reported in Table 4. For the export cables that link the offshore substation with the onshore electricity delivery point, both variable costs, which depend on the length of the cable, and fixed costs, which account for the electrical substructures needed independently of distance, were considered. To estimate the CAPEX (Equation 4) of the moorings, the approach proposed by Heidari et al. [37], which considers

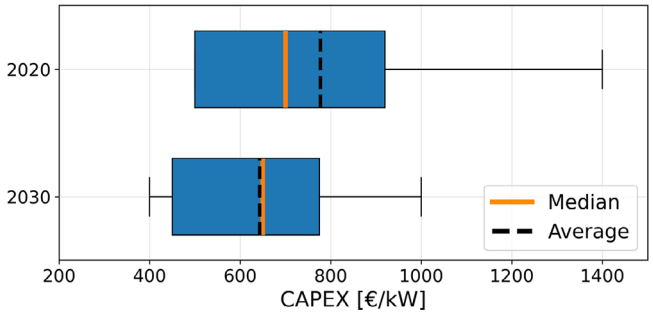

FIGURE 5 ALK electrolyzers CAPEX at 2020 and at 2030.

the minimum breaking load (BL), the length (L) of the catenary, and the number of moorings per turbine (N), was used.

$$\mathrm{CAPEX}_m = \mathrm{N} * [(0.0591 * \mathrm{BL} - 87.69) * \mathrm{L} + 10.198 * \mathrm{BL}]. \quad (4)$$

Moreover, to accurately evaluate the expenditure, the correct estimation of the length of the catenary is crucial. The approach proposed by Martinez et al. in [23], which estimates a length of 560 m for a sea depth of 100 m and an additional 150 m for every 100 m depth at the installation site, results in a total length of 900 m for each mooring line. Finally, the cost of turbine and platform installations was scaled with respect to that reported by NREL in [42] for wind farms with a capacity of 600 MW. Regarding electrolyzers, to account for projections to 2030, a sensitivity analysis was conducted. Regardless of the size of the plant, the CAPEX of electrolyzers was set to three different values, that is, 500, 750, and 1000€/kW, as detailed in [43]. These values were selected based on the extensive amount of data available in the literature, which has been summarized in a box and whisker plot (Figure 5). In this plot, a box spans from the first to the third quartile, with a vertical solid line representing the median value and a vertical dashed line indicating the average value. The chosen values for the sensitivity analysis are included within the boxes and are likely to be the most representative for a projection up to 2030. Additionally, according to the literature [9], a stack lifetime of ten years was assumed, leading to two substitutions of the component during the wind farm lifetime. This assumption is consistent with the evaluation of a degradation lower than 20% of the nominal performance after 10 years of operation. Considering that the stack contains the most expensive components, the replacement costs were set at 40% of the capital expenditure for the electrolyzer. Moreover, for this component, the cost is evaluated from a reference cost C_0 and a reference size x_0, which is then scaled to the actual component size x via a scale factor equivalent to 0.69 [44], as depicted in (Equation 5).

$$\mathrm{CAPEX}_{\mathrm{electrolyser}} = C_0 * \left(\frac{x}{x0}\right)^{0.69}. \quad (5)$$

Defining the OPEX of floating wind technology is even more challenging. Maintenance operations required for floating wind farms are still largely unknown, although it can be reasonably

TABLE 5 AEP of the analyzed wind farm layouts.

Farm layout	10 MW WTs farm [GWh/y]	15 MW WTs farm [GWh/y]
Square 5d-5d	2313,0	2458,5
Square 7d-7d	2679,4	2844,9
Rectangular 10d-5d	2687,4	2859,4
Rectangular 10d-7d	2789,5	2976,0
Square 10d-10d	2833,9	3013,9

expected that they will be more complex and expensive compared to fixed-bottom farms. In this study, an OPEX value equivalent to 5% of the capital cost was adopted. For the hydrogen production system, the operation and maintenance costs were assumed to be equal to 5.5% of the capital expenditure.

3 | RESULTS

This section presents an overview of the wind farm results for the analyzed scenario in terms of AEP, wake losses, and capacity factors to highlight the effects of the phenomena included in the model. As discussed, the wind farm size was held constant at 1 GW, while hydrogen production was simulated with electrolyzer nominal powers ranging from 10 to 60 MW. This parametric analysis enables the evaluation of the best plant configuration for each curtailment scenario.

3.1 | AEP

As discussed, a good LCOE estimation needs an accurate prediction of the AEP. This section shows the results in terms of energy production, considering aerodynamic losses and downtime periods due to maintenance. Upon examination of Table 5, it is apparent that the AEP of the 15 MW WTs farm is higher than the 10 MW WTs farm in every layout. This is due to several factors, including the greater hub height and a 0.5% higher installed capacity of the 15 MW farm, achieved through the installation of 67 wind generators to reach the nominal power. Furthermore, despite the higher wake losses observed in Figure 6, the increased swept area leads to better exploitation of lower wind speeds, resulting in higher capacity factors (Figure 7). Table 5 also emphasizes the dependence of the AEP on the farm layout. As expected, both farms show a higher AEP with the increase in turbine distance due to the reduced wake losses. Switching from a 5d-5d to a 7d-7d layout allows for the highest increase in AEP (approx. 15%), while the adoption of a 10d-10d layout results in smaller improvements, as confirmed by the capacity factors shown in Figure 7.

3.2 | LCOE

This section presents the results of the economic analysis, highlighting the variations in the LCOE induced by a variable

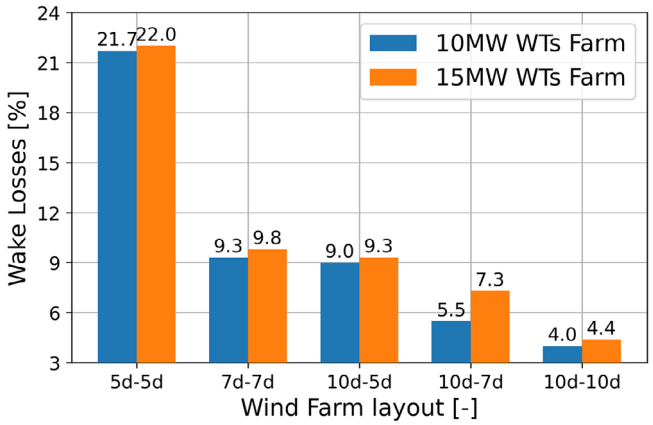

FIGURE 6 Wake losses of the analyzed wind farm layouts.

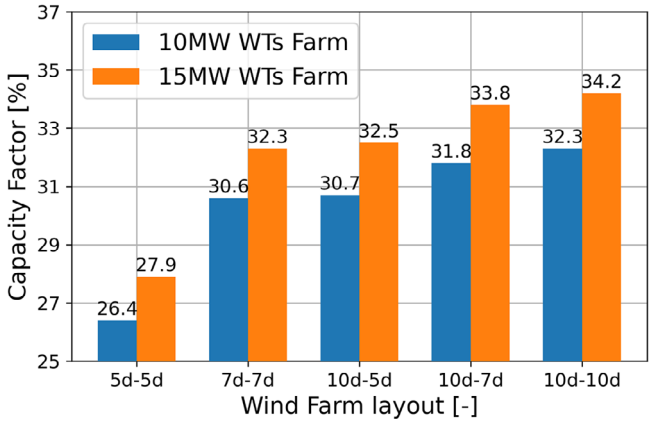

FIGURE 7 Capacity factor of the analyzed wind farm layouts.

TABLE 6 LCOE [€/MWh] of the 10 MW WTs farm.

Farm layout	$i = 5\%$	$i = 7\%$	$i = 9\%$
Square 5d-5d	140.5	159.4	179.9
Square 7d-7d	122.7	139.3	157.2
Rectangular 10d-5d	121.4	137.8	155.4
Rectangular 10d-7d	118.1	134.0	151.2
Square 10d-10d	118.1	134.1	151.3

interest rate (i). As i represents the level of trust of investors in a project, a parametric study is needed due to the challenges induced in the forecasts for an analysis starting from 2030. An increase in the interest rate results in a rise in the LCOE, as shown in both Tables 6 and 7. The techno-economic analysis results demonstrate that an increase in AEP is not necessarily related to a decrease in energy costs. Despite the reduction of wake losses induced by increasing turbine distance, the increases in CAPEX and OPEX cause a higher LCOE, as shown with the 10d-10d layout for the 10 MW WTs farm.

On the other hand, regarding the 15 MW configuration, the increase in turbine distance highlights the convenience of the squared layout, as testified by Table 7. Furthermore, a

TABLE 7 LCOE [€/MWh] of the 15 MW WTs farms.

Farm layout	$i = 5\%$	$i = 7\%$	$i = 9\%$
Square 5d-5d	129.4	146.8	165.7
Square 7d-7d	112.9	128.2	144.6
Rectangular 10d-5d	113.4	128.7	145.2
Rectangular 10d-7d	110.2	125.1	141.1
Square 10d-10d	108.2	122.9	138.6

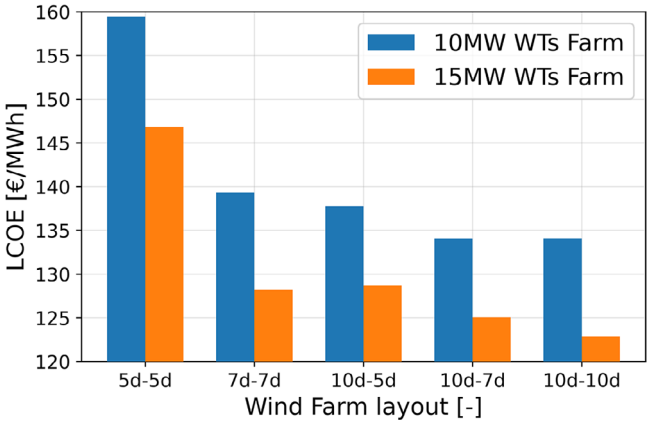

FIGURE 8 LCOE of the analyzed wind farms (i = 7%).

comparison can be made between the two different farms. The 15 MW configurations, as shown in the tables below and in the bar plot of Figure 8, are always characterized by a lower LCOE due to the lower investment costs and higher AEP. These results can be compared with the ones obtained in previous studies by RSE. In that case, the use of the Weibull curve and a simplified wake model resulted in different LCOEs. Given the higher approximations used, these values range from 95 to 121€/MWh and from 92 to 118€/MWh, for the 10MW and the 15MW, respectively. Furthermore, the findings proposed by this study are consistent with the outcomes shown by previous works. LCOE for floating offshore wind farms in the Mediterranean Sea ranges from 130 to 180€/MWh, depending on the installation areas and on the technologies adopted [23].

3.3 | LCOH

Based on the results of Section 3.2, the 10d-7d and 10d-10d layouts were chosen for the 10 MW and 15 MW WTs farms, respectively, to investigate the cost of possible green hydrogen production. It is worth noticing that the present study does not consider any cost related to hydrogen storage and transport; the following results must then be considered as only related to hydrogen production cost. As previously mentioned, curtailments were accounted as a fixed percentage of the AEP for every hour of the year (S1) and with a distribution to consider grid congestion throughout the day (S2). As discussed, the comparison between those two approaches allows one to estimate

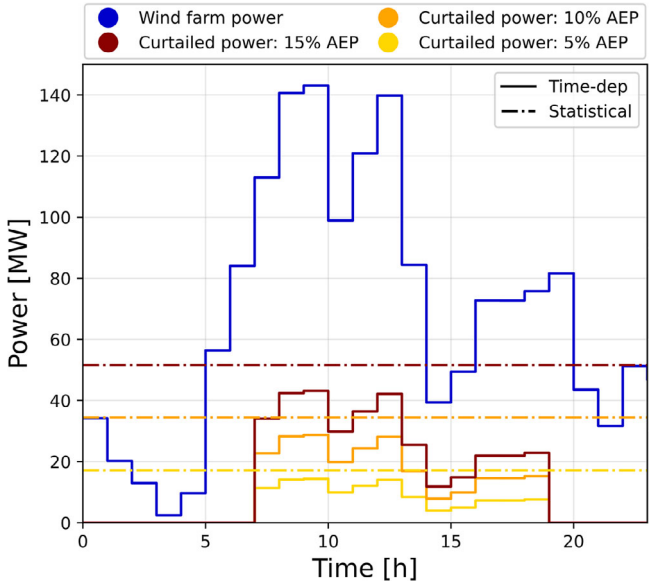

FIGURE 9 Power production and curtailed power for the time-dependent and statistical approach, in all curtailment scenarios.

the limitations of the common practice for preliminary analyses (S1). To this end, Figure 9 shows the comparison between the different curtailment distributions during 24 h of simulation.

A statistical approach like the one used in S1 translates, in the time domain, in a constant power input available for the electrolyzer. Therefore, even during a day on non-constant production form the wind farm as the one shown in the image, S1 would still consider a constant power input to the electrolysis facility, leading to an overestimation of the CF of the component. On the other hand, S2 results in a more realistic power input estimation, also due to the clustering of curtailments during the central hours of the day, when the probability of going through grid congestions is higher. Even if the total curtailed energy is equivalent both in S1 and S2, the time distribution of the available energy affects the estimation of the hydrogen production.

Indeed, during a day of low production as the one shown in Figure 9, S1 shows a higher curtailment power throughout the whole day for all curtailment scenarios.

Figure 10 highlights, time-step per time-step, the differences between S1 and S2 in the scenario characterized by the higher curtailed energy in the same 24 h of Figure 9. In detail, the grey area represents the difference in energy available for the electrolyzer. S1 leads to a relevant overestimation of the curtailed energy in the off-peak hours, while in S2 all the wind farm power is fed into the grid. As highlighted by the hatched light grey area in the plot, this trend may result in energy availability even larger than the wind farm production. Those two aspects, combined with the constant power input to the electrolysis facility, result in an underestimation of the LCOH, as described in this section.

Two different economic scenarios were considered. In the first scenario (referred to as "LCOH low"), a hypothetical future projection, more likely to happen after 2030, is considered in which the curtailed energy is not valued and can be then used

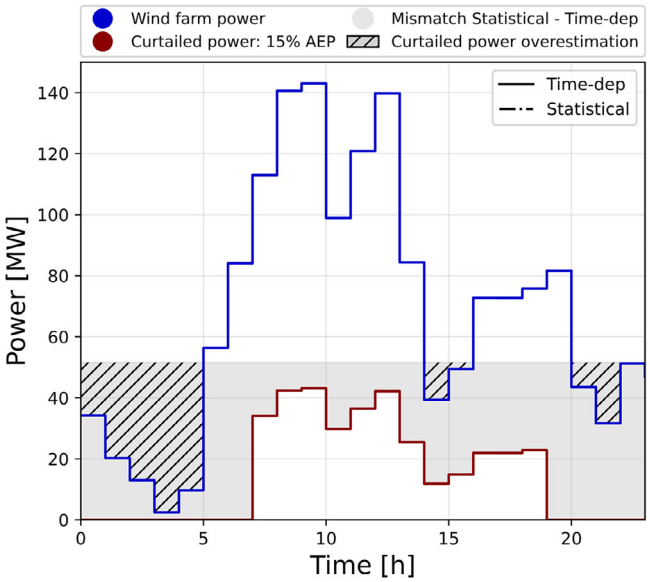

FIGURE 10 Power production and curtailed power for the time-dependent and statistical approach, the 15% AEP curtailment scenario.

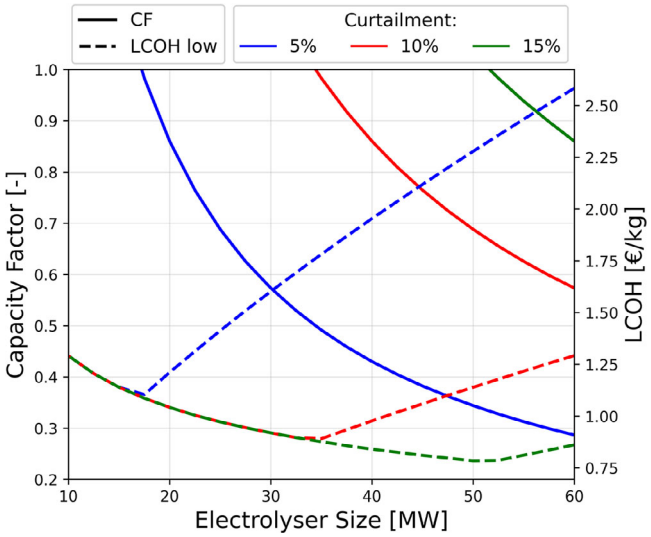

FIGURE 11 LCOH and capacity factors in S1 for different curtailment magnitudes for the 15 MW WTs farm and an electrolyzer plant with CAPEX of 1000€/kW.

TABLE 8 Curtailment scenarios simulated.

Curtailment scenario		Economic scenario
S1	5% AEP	LCOH low: 0%LCOE LCOH high: 50% LCOE
	10% AEP	
	15% AEP	
S2-a: 12 h S2-b: 24 h	5% AEP	LCOH low: 0%LCOE LCOH high: 50% LCOE
	10% AEP	
	15% AEP	

by the electrolyzer at no cost. The second scenario (referred to as "LCOH high") is instead more closely linked to the actual one, in which the curtailed energy is valued to the producers. In the study, it is figured out that a tariff of 50% of the LCOE is granted to the wind farm, which translates into a cost of energy sold to the electrolysis system equal to half of the energy production cost. Finally, in S2-b since the additional energy is not due to curtailments, it is valued as the LCOE. Table 8 summarizes the scenarios and plant configurations tested.

In order to quantify the equivalent annual operating hours of the electrolysis plant, the CF is calculated:

- in S1, as the ratio of the whole available input energy from curtailments and the maximum producibility of the electrolyzer.
- in S2, as the ratio between the hydrogen actually produced by the electrolyzer according to the time-dependent calculation, and the maximum producibility of the electrolyzer.

3.3.1 | Statistical approach

Figure 11 shows the dependence of the LCOH and the CF in S1 on the size of the electrolyzers while varying the energy input; results refer to the 15 MW wind farm and an electrolysis plant with a specific cost of 1000€/kW in the LCOH low scenario. As a consequence of the excess available energy compared to the installed capacity of electrolyzers, in S1 the CF may assume values greater than one. To this end, as shown in the plot, an upper limit of one has been set to be consistent with the standard practice adopted in the literature for this metric.

Conversely, a lower CF is due to an oversized plant if compared to the curtailed energy. According to this, the CF equivalent to 1 can be used as a target to be met for the economic optimization of the plant. Therefore, the LCOH increases as the electrolyzer capacity decreases or increases with respect to the optimal size. As shown by Figure 11, the minimum hydrogen production price in the LCOH low scenario is equivalent to 1.1, 0.89, and 0.79€/kg for curtailed energy values of 5%, 10%, and 15%, respectively, due to the higher hydrogen production without any changes in the plant CAPEX. Moreover, the optimal hydrogen costs are obtained with an installed electrolyzer capacity of 17.5, 30, and 50 MW, respectively. In the case of the 10 MW WTs farm layout, for the same percentage of curtailment, the energy designed to supply the electrolysis plant is lower. Under these conditions, the minimum hydrogen costs obtained are 1.14, 0.96, and 0.79€/kg, respectively. Furthermore, a difference can be observed also in the optimal plant size, which is 2.5 MW lower for each curtailment scenario, as shown in Table 9.

Regarding the LCOH high scenario, Figure 12 shows that the optimal configuration is reached for the same electrolyzer sizes, due to the unchanged CF.

From this plot and from Table 10, it is apparent that the 15 MW farm leads to minimum LCOH of 4.11, 3.9, and 3.79€/kg. Focussing on the comparison between the LCOH low and high scenarios, some similarities can be noticed. For sizes lower than the optimal one the LCOH trends collapse on the same value, disregarding the available energy. This trend is due to the limit to the utilization of the energy set by the

TABLE 9 LCOH for optimal electrolyzer capacities for the 10 and 15 MW WTs farm in the LCOH low scenario.

Wind farm	Curtailment scenario	Optimal electr. size [MW]	LCOH [€/kg]
15 MW WTs	5% AEP	17.5	1.1
	10% AEP	30	0.89
	15% AEP	50	0.79
10 MW WTs	5% AEP	13	1.14
	10% AEP	24	0.96
	15% AEP	32	0.79

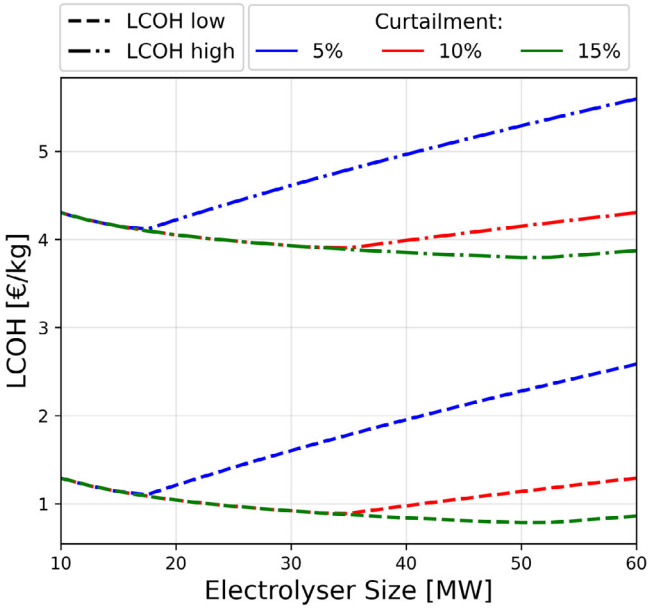

FIGURE 12 LCOH comparison between the LCOH low and high scenario for the 15 MW WTs farm and an electrolyzer CAPEX of 1000€/kW in the LCOH high scenario.

TABLE 10 LCOH for optimal electrolyzer capacities for the 15 MW WTs farm in the LCOH high scenario.

Wind farm	Curtailment scenario	Optimal electr. size [MW]	LCOH [€/kg]
15 MW WTs	5% AEP	17.5	4.11
	10% AEP	30	3.90
	15% AEP	50	3.79

electrolyzer size, which results in an equivalent hydrogen production. Sub-optimal electrolyzer sizes thus correspond to an exploitation of energy lower than the available one. On the other hand, oversized electrolyzers lead to a higher LCOH. This dependence increases reducing the curtailed energy, given the increased mismatch between the available power and the electrolyzer size. However, while the trend described by the two series is equivalent, the LCOH of the scenario where energy

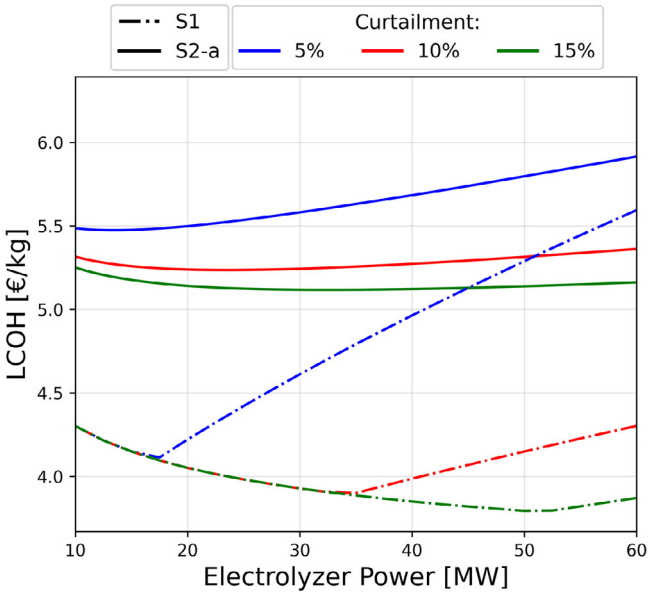

FIGURE 13 LCOH comparison between the statistical and time-dependent case for the 15 MW WTs farm and an electrolyzer CAPEX of 1000€/kW in the LCOH high scenario.

TABLE 11 CF and LCOH for optimal electrolyzer capacities in different curtailment scenarios.

Curtailment scenario	Optimal electr. size [MW]	CF [%]	LCOH [€/kg]
5% AEP	13	34	5.47
10% AEP	24	35	5.23
15% AEP	32	36	5.12

is not valued is shifted downwards due to the lower operational costs.

3.3.2 | Comparison statistical–time-dependent

Figure 13 depicts the comparison between the results obtained for the LCOH high scenario in the statistical (S1: dashed lines) and time dependent approach (S2-a: solid lines) varying the electrolyzer capacity. From this plot, it is apparent that considering the real availability of the input power to the electrolysis plant leads to higher LCOH and lower optimal capacities. In detail, the minimum LCOH and the optimal sizes associated with curtailments of 5%, 10%, and 15% of the estimated AEP in S2-a are reported in Table 11.

Furthermore, the time-dependent approach leads to a different trend at lower electrolyzer capacities. Specifically, despite the reduced difference in LCOH, the values do not collapse. The increase in the available energy is thus related to an enhanced exploitation of curtailed power and hydrogen production.

Additionally, a key point to emphasize is that the S2-a scenario experiences a lower sensitivity to the electrolyzer size with

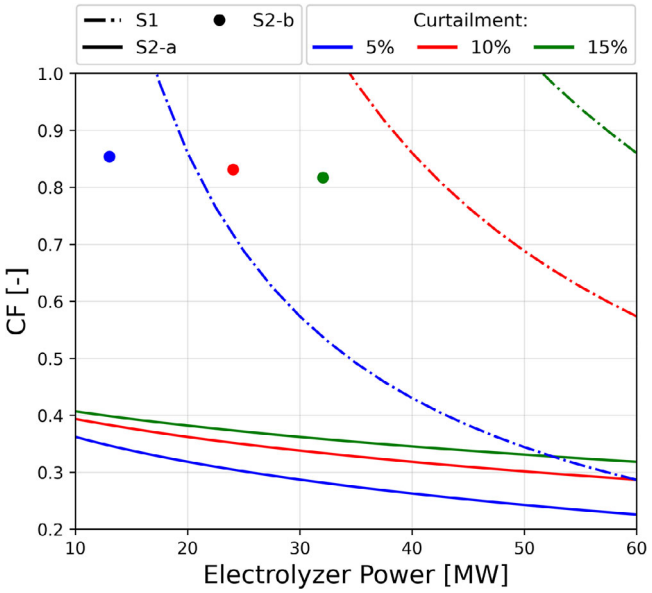

FIGURE 14 CF in the time-dependent case for the 15 MW WTs farm and an electrolyzer CAPEX of 1000€/kW.

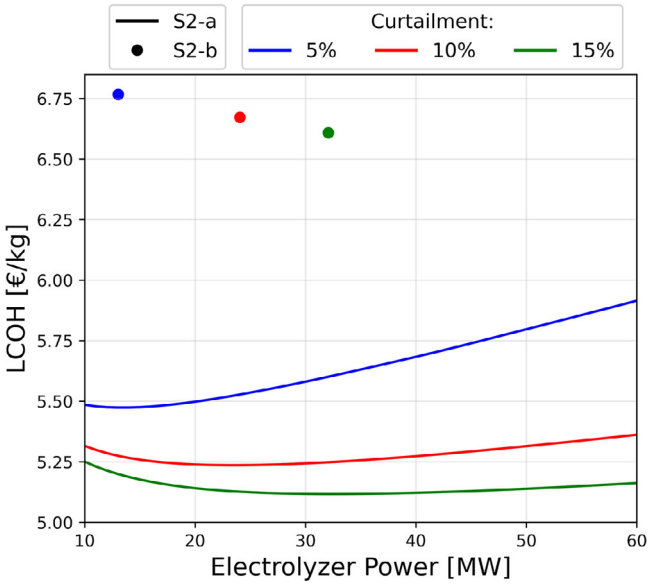

FIGURE 15 LCOH comparison between the 12 and 24 h time-dependent case for the 15 MW WTs farm and an electrolyzer CAPEX of 1000€/kW in the LCOH high scenario.

respect to the statistical approach. This is due to the distribution of the curtailed energy throughout the year. Accounting for the availability of energy at a specific time step during the simulation results in a lower dependency on the electrolyzer size, as testified by the reduced variability of the CF shown in Figure 14. This trend is the result of different curtailment distributions. While in S1 the hourly power designed for hydrogen production is distributed equally for the whole year, S2-a and b account for the real wind farm power production. For these reasons, the CF equivalent to 1 can be used as a target for the LCOH minimization only in the first case, when the optimal electrolyzer capacity matches the available hourly power (Figure 9). As expected, in S2-a CFs are lower (Figure 14, solid lines) and the trade-off between the increase in hydrogen production and in the electrolyzer CAPEX is reached at lower capacities. However, while further reductions in electrolysis plant size would increase the CF, those are associated with a decrease in hydrogen production higher than the one in investment costs. Figure 14 emphasizes the CF overestimation in S1 by comparing this scenario with S2.

In detail, the dots in the figure represent a 'hydrogen-driven' scenario where the optimal capacities obtained in S2-a are utilized to define a constant power withdrawal from the wind farm. To this end, S2-b aims to reduce the LCOH through the maximization of CFs with better exploitation of wind power. Despite the attempt to feed the electrolyzers with the nominal power input, the wind power availability obtained by the simulations leads to maximum CFs lower than one in all curtailment configurations. This parameter can be used to estimate the mismatch between the expected production, represented by the statistical approach, and the nominal electrolyzer producibility. Furthermore, a decrease in CF with the curtailment energy available is shown in the plot for the S2-b scenario. This is due to an increase in power availability higher than the one in energy exploited for hydrogen production.

Figure 15 shows the comparison between the results of S2-a (solid lines) and S2-b (dots) in terms of hydrogen production costs. Despite the increase in CF, the high pricing of the energy in addition to that from curtailments in the S2-b causes an increase in LCOH in all curtailment scenarios. In detail, LCOH is equivalent to 6.77€/kg, 6.67€/kg, and 6.61€/kg in the curtailment scenarios at 5%, 10%, and 15%, respectively. These results are consistent with the 5.9$/kg and 3.77€/kg shown in [5, 6], respectively, where hydrogen is produced from curtailments. However, the present analysis does not estimate the real convenience of adopting a hydrogen-driven configuration. To this aim, only accounting for hydrogen selling price in the economic analysis would allow to estimate if the S2-b configuration is economically more attractive.

As expected, the curtailment scenario characterized by the higher energy available to the electrolyzer experiences lower LCOH in both S2-a and S2-b. This is due to higher hydrogen production, as shown in Figure 16. As a final remark, one last consideration can be made on the hydrogen production throughout the plant's lifetime.

Figure 16 shows how, while the increase in the available energy leads to a proportional increase in hydrogen production in the statistical scenario, in S2-a and S2-b the time-dependent distribution of curtailments results in a sublinear dependency on available power. This is consistent with the results in terms of CF, where an increase in available energy does not correspond to a proportional increase in the electrolyzer operational time. Finally, while S2-a shows an increase in hydrogen production with the electrolyzer size, S1 arrives soon at saturation once the optimal size is reached. This is due to the exploitation of all the curtailed energy and an increase in the installed power of the electrolysis facility does not affect the production. This trend is consistent with the sudden increase in the LCOH shown in Figure 13.

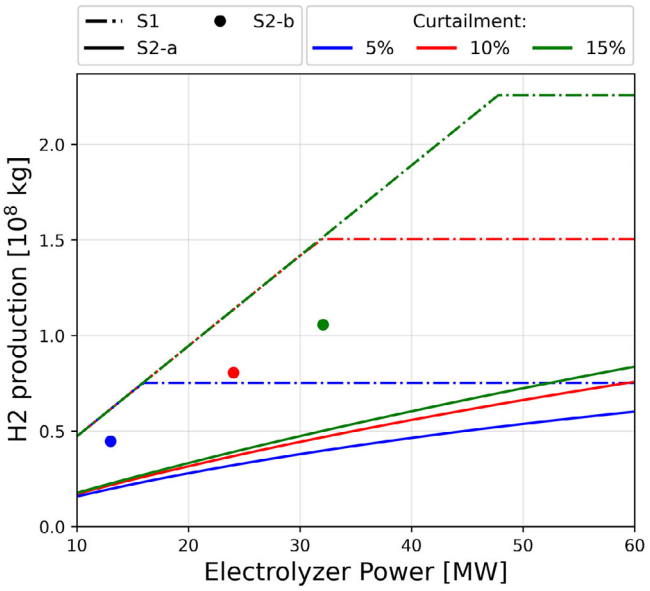

FIGURE 16 Hydrogen production comparison between the 12 and 24 h time-dependent for the 15 MW WTs farm and an electrolyzer CAPEX of 1000€/kW in the LCOH high scenario.

4 | CONCLUSIONS

In this study, a computational framework is implemented and applied to evaluate the producibility of an offshore wind farm coupled with a hydrogen production system near the Sardinian shores in Italy. The use of historical wind speed and direction time series allows to introduce a farm model that directly estimates wake effects, which improves the accuracy of the simulated AEP. The developed framework was then used to compute the LCOE of floating wind farms, as well as a first estimation of the LCOH of possible green hydrogen production within curtailment periods, so as to provide reference data for techno-economic analyses in the Mediterranean Sea.

First, the AEP of different floating wind farm configurations was evaluated. As expected, it was shown that a delicate balance must be pursued when using this technology. When the distance between wind turbines is increased, the AEP obviously improves as a result of milder wake losses, but the very high costs of electrical connections define an optimal value of the distance, even in the case where no space limitation is given.

Overall, it was estimated that for the selected case study, LCOE will range between 108 and 165€/MWh for a farm using 15 MW turbines, and between 118 and 180€/MWh for a farm using 10 MW turbines.

Regarding the LCOH of green hydrogen produced in response to curtailments imposed by the grid, different considerations can be made. Under the relevant assumption of considering no energy cost in input to the electrolyzer, it was found that LCOH ranges between 0.71€/kg and 2.32€/kg for a farm using 15MW turbines, and between 0.72€/kg and 2.51€/kg for a farm using 10 MW turbines if just the aggregated result is accounted for. Applying a historic time series to estimate the hourly curtailed energy, simulating a more realistic scenario, the results have shown an increase in hydrogen production costs, ranging between 5.12€/kg and 6.27€/kg if curtailments are priced 50% of the LCOE. Although the statistical approach shows more cost-effective outcomes, it is unsuitable for a real test case since it does not take into account the actual availability of the resource. However, this model does not take into account a detailed modeling for the electrolyzer, neglecting parameters such as startups and shutdowns of the component and the degradation related to the intermittent operation of the electrolysis facility. Despite the relevance of those parameters to assess the realistic behavior of the electrolyzer, the adoption of an hourly timestep reduces the impact of the choice on the accuracy of the analysis. Finally, assuming a configuration where hydrogen demand is the driver of the analysis and the energy in addition to that curtailed is paid as the LCOE, LCOH increases up to values of 6.77€/kg. These results can influence policymakers by demonstrating the cost-effectiveness and reliability of FOWTs coupled with electrolyzers to produce green hydrogen as a way to reduce energy waste due to curtailments. Supportive regulations, subsidies, and incentives that promote the adoption of these technologies can be developed, accelerating the achievement of the energy targets set by Mediterranean Countries.

Future models could further improve the economic analysis, considering hydrogen selling prices to estimate the real convenience of the hydrogen-driven scenario instead of considering hydrogen as a side product of the system.

AUTHOR CONTRIBUTIONS

Riccardo Travaglini: Data curation; formal analysis; investigation; methodology; software; writing—original draft. **Francesco Superchi**: Investigation; methodology; software; writing—review and editing. **Francesco Lanni**: Methodology; resources; supervision; writing—review and editing. **Giovanni Manzini**: Supervision; writing—review and editing. **Laura Serri**: Conceptualization; funding acquisition; project administration; resources; writing—review and editing. **Alessandro Bianchini**: Conceptualization; funding acquisition; investigation; methodology; project administration; supervision; writing—review and editing.

ACKNOWLEDGEMENTS

This work has been financed by the Research Fund for the Italian Electrical System under the Three-Year Research Plan 2022–2024 (DM MITE n. 337, 15.09.2022), in compliance with the Decree of April 16th, 2018.

CONFLICT OF INTEREST STATEMENT

The authors declare no conflicts of interest.

DATA AVAILABILITY STATEMENT

Data are available upon request to the contact author.

ORCID

Riccardo Travaglini https://orcid.org/0009-0008-2236-272X
Francesco Superchi https://orcid.org/0000-0001-5514-0869
Alessandro Bianchini https://orcid.org/0000-0002-8042-5863

REFERENCES

1. Zountouridou, E.I., Kiokes, G.C., Chakalis, S., Georgilakis, P.S., Hatziargyriou, N.D.: Offshore floating wind parks in the deep waters of Mediterranean Sea. Renew Sustain. Energy Rev. 51, 433–448 (2015). https://doi.org/10.1016/j.rser.2015.06.027
2. WindEurope. Floating Offshore Wind Vision Statement. WindEurope (2017). https://windeurope.org/about-wind/reports/floating-vision-statement/. Accessed 3 Jan 2023
3. Superchi, F., Mati, A., Carcasci, C., Bianchini, A.: Techno-economic analysis of wind-powered green hydrogen production to facilitate the decarbonization of hard-to-abate sectors: A case study on steelmaking. Appl. Energy 342, 121198 (2023). https://doi.org/10.1016/j.apenergy.2023.121198
4. Wang, D., Muratori, M., Eichman, J., Wei, M., Saxena, S., Zhang, C.: Quantifying the flexibility of hydrogen production systems to support large-scale renewable energy integration. J. Power Sources 399, 383–391 (2018). https://doi.org/10.1016/j.jpowsour.2018.07.101
5. Park, J., Hwan Ryu, K., Kim, C.-H., Chul Cho, W., Kim, M., Hun Lee, J., et al. Green hydrogen to tackle the power curtailment: Meteorological data-based capacity factor and techno-economic analysis. Appl. Energy 340, 121016 (2023). https://doi.org/10.1016/j.apenergy.2023.121016
6. McDonagh, S., Ahmed, S., Desmond, C., Murphy, J.D.: Hydrogen from offshore wind: Investor perspective on the profitability of a hybrid system including for curtailment. Appl. Energy 265, 114732 (2020). https://doi.org/10.1016/j.apenergy.2020.114732
7. Biggins, F.A.V., Ejeh, J.O., Roberts, D., Yeardley, A.S., Brown, S.F.: Optimising a wind farm with energy storage considering curtailment and uncertainties. In: Montastruc L., Negny S., (eds.) Computer Aided Chemical Engineering, vol. 51, pp. 79–84. Elsevier, Amsterdam (2022). https://doi.org/10.1016/B978-0-323-95879-0.50014-X
8. Yan, X., Zhang, X., Gu, C., Li, F.: Power to gas: Addressing renewable curtailment by converting to hydrogen. Front Energy 12, 560–568 (2018). https://doi.org/10.1007/s11708-018-0588-5
9. Gambou, F., Guilbert, D., Zasadzinski, M., Rafaralahy, H.: A comprehensive survey of alkaline electrolyzer modeling: Electrical domain and specific electrolyte conductivity. Energies 15, 3452 (2022). https://doi.org/10.3390/en15093452
10. Falcão, D.S., Pinto, A.M.F.R.: A review on PEM electrolyzer modelling: Guidelines for beginners. J Clean Prod 261, 121184 (2020). https://doi.org/10.1016/j.jclepro.2020.121184
11. Ministero dello Sviluppo Economico. Piano Nazionale Integrato per l'Energia e il Clima (2019)
12. Mehta, M., Zaaijer, M., von Terzi, D.: Drivers for optimum sizing of wind turbines for offshore wind farms. Wind Energy Sci. 9, 141–163 (2024). https://doi.org/10.5194/wes-9-141-2024
13. Wind Europe: Repowering and Lifetime Extension: making the most of Europe's wind resource (2017)
14. IEA Wind TCP Task 42. IEA Wind TCP 2022. https://iea-wind.org/task42/. Accessed 26 Feb 2024
15. Ghigo, A., Cottura, L., Caradonna, R., Bracco, G., Mattiazzo, G.: Platform optimization and cost analysis in a floating offshore wind farm. J. Mar. Sci. Eng. 8, 835 (2020). https://doi.org/10.3390/jmse8110835
16. Ramirez Gonzalez, L.: 2050: Power-to-hydrogen opportunities for far offshore wind farms. Master thesis, Delft University of Technology (2018)
17. Ramachandran, R.C., Cian, D., Frances, J., Jorrit-Jan, S., Jimmy, M.: Floating wind turbines: Marine operations challenges and opportunities. WES 7(2), 903–924 (2022). https://doi.org/10.5194/wes-7-903-2022
18. COREWIND: D3.1 Review of the state of the art of dynamic cable system design (2020)
19. Ardelan, M., Minnebo, P.: HVDC Submarine Power Cables in the World. European Commission, Brussels, Belgium (2015)
20. RSE: L'energia elettrica dal vento, RSEview (2017)
21. Timmers, V., Egea-Alvarez, A., Gkountaras, A., Li, R., Xu, L.: All-DC offshore wind farms: When are they more cost-effective than AC designs? IET Renew. Power Gener. 17(10), 2458–2470 (2022). https://doi.org/10.1049/rpg2.12550
22. Jiang, Q., Li, B., Liu, T.: Tech-economic assessment of power transmission options for large-scale offshore wind farms in China. Processes 10, 979 (2022). https://doi.org/10.3390/pr10050979
23. Martinez, A., Iglesias, G.: Multi-parameter analysis and mapping of the levelised cost of energy from floating offshore wind in the Mediterranean Sea. Energy Convers. Manag. 243, 114416 (2021). https://doi.org/10.1016/j.enconman.2021.114416
24. Ibrahim, O.S., Singlitico, A., Proskovics, R., McDonagh, S., Desmond, C., Murphy, J.D.: Dedicated large-scale floating offshore wind to hydrogen: Assessing design variables in proposed typologies. Renew Sustain. Energy Rev. 160, 112310 (2022). https://doi.org/10.1016/j.rser.2022.112310
25. RSE: AEOLIAN. https://atlanteeolico.rse-web.it/. Accessed 19 Apr 2023
26. Hersbach, H., Bell, B., Berrisford, P., Hirahara, S., Horányi, A., Muñoz-Sabater, J., et al.: The ERA5 global reanalysis. Quart. J. Royal Meteorol. Soc. 146, 1999–2049 (2020). https://doi.org/10.1002/qj.3803
27. EMD International: windPRO 3.6 User Manual: Energy (2022)
28. Lundtang Petersen, E., Troen, I., Ejsing Jørgensen, H., Mann, J.: The new European wind atlas. Energy Bull. 34–39 (2014)
29. Katic, I., Højstrup, J., Jensen, N.O.: A simple model for cluster efficiency. In: European Wind Energy Association Conference and Exhibition, EWEC86, vol. 1, pp. 407–410. European Wind Energy Association, Brussels, Belgium (1987)
30. Morten Lybech, T.: Introduction to wind turbine wake modelling and wake generated turbulence (2021)
31. Sørensen, T., Lybech Thøgersen, M., Nielsen, P.H.: Adapting and calibration of existing wake models to meet the conditions inside offshore wind farms. Technical Report, EMD International, Aalborg (2008)
32. Pratt, R.: A Comparison of the observed wake effect with several wake models using both analytic and cfd simulation methods-for the case of block island offshore wind farm (2019)
33. Terna: Documento di Descrizione degli Scenari 2022 (2022). https://www.terna.it/it/sistema-elettrico/rete/piano-sviluppo-rete/scenari. Accessed 19 Apr 2023
34. Record-breaking hydrogen electrolyzer claims 95% efficiency. New Atlas (2022). https://newatlas.com/energy/hysata-efficient-hydrogen-electrolysis/. Accessed 19 Apr 2023
35. Superchi, F., Papi, F., Mannelli, A., Balduzzi, F., Ferro, F.M., Bianchini, A.: Development of a reliable simulation framework for techno-economic analyses on green hydrogen production from wind farms using alkaline electrolyzers. Renew Energy 207, 731–742 (2023). https://doi.org/10.1016/j.renene.2023.03.077
36. Sethuraman, L., Maness, M., Dykes, K.: Optimized generator designs for the DTU 10-MW offshore wind turbine using GeneratorSE (2017). https://doi.org/10.2514/6.2017-0922
37. Heidari, S.: Economic modelling of floating offshore wind power: Calculation of levelized cost of energy (2017)
38. Markus, L.: Expected LCOE for floating wind turbines 10MW+ for50m+ water depth (2019). https://ec.europa.eu/research/participants/documents/downloadPublic?documentIds=080166e5c3ac71f4&appId=PPGMS. Accessed 20 Apr 2023
39. Lerch, M., De-Prada-Gil, M., Molins, C.: A metaheuristic optimization model for the inter-array layout planning of floating offshore wind farms. Int. J. Electr. Power Energy Syst. 131, 107128 (2021). https://doi.org/10.1016/j.ijepes.2021.107128
40. Fjellstedt, C., Ullah, M.I., Forslund, J., Jonasson, E., Temiz, I., Thomas, K.: A review of AC and DC collection grids for offshore renewable energy with a qualitative evaluation for marine energy resources. Energies 15, 5816 (2022). https://doi.org/10.3390/en15165816
41. Johannes, P.P., John, T., Samuel, A.N, The benefit and cost of preserving the option to create a meshed offshore grid for New York (2021). https://www.brattle.com/wp-content/uploads/2021/12/The-Benefit-and-Cost-of-Preserving-the-Option-to-Create-a-Meshed-Offshore-Grid-for-New-York.pdf. Accessed 19 Apr 2023
42. Beiter, P., Musial, W., Smith, A., Kilcher, L., Damiani, R., Maness, M., et al.: A spatial-economic cost-reduction pathway analysis for U.S.

Offshore Wind Energy Development from 2015–2030. National Renewable Energy Lab. (NREL), Golden, CO (2016). https://doi.org/10.2172/1324526
43. Idrogeno—Un vettore energetico per la decarbonizzazione. https://www.rse-web.it/prodotti_editoriali/idrogeno_rseview/. Accessed 19 Apr 2023
44. Lehmann, J., Wabbes, A., Miguelañez Gonzalez, E., Scheerlinck, S.: Levelized cost of hydrogen calculation from off-grid photovoltaic plants using different methods. Sol. RRL 6, 2100482 (2022). https://doi.org/10.1002/solr.202100482

How to cite this article: Travaglini, R., Superchi, F., Lanni, F., Manzini, G., Serri, L., Bianchini, A.: Towards the development of offshore wind farms in the Mediterranean Sea: A techno-economic analysis including green hydrogen production during curtailments. IET Renew. Power Gener. 1–15 (2024). https://doi.org/10.1049/rpg2.13135